

Investigation of the effects of temperature on the microstructure of PTFE microfiltration membranes under membrane distillation conditions

Citation for published version:

Hughes, AJ, Mallick, TK & O'Donovan, TS 2020, 'Investigation of the effects of temperature on the microstructure of PTFE microfiltration membranes under membrane distillation conditions', *Journal of Advanced Thermal Science Research*, vol. 7, pp. 11-21. <https://doi.org/10.15377/2409-5826.2020.07.2>

Digital Object Identifier (DOI):

[10.15377/2409-5826.2020.07.2](https://doi.org/10.15377/2409-5826.2020.07.2)

Link:

[Link to publication record in Heriot-Watt Research Portal](#)

Document Version:

Publisher's PDF, also known as Version of record

Published In:

Journal of Advanced Thermal Science Research

General rights

Copyright for the publications made accessible via Heriot-Watt Research Portal is retained by the author(s) and / or other copyright owners and it is a condition of accessing these publications that users recognise and abide by the legal requirements associated with these rights.

Take down policy

Heriot-Watt University has made every reasonable effort to ensure that the content in Heriot-Watt Research Portal complies with UK legislation. If you believe that the public display of this file breaches copyright please contact open.access@hw.ac.uk providing details, and we will remove access to the work immediately and investigate your claim.

Investigation of the Effects of Temperature on the Microstructure of PTFE Microfiltration Membranes Under Membrane Distillation Conditions

A.J. Hughes^{1,*}, T.K. Mallick² and T.S. O'Donovan³

¹*School of Engineering, University of Liverpool, Liverpool, L69 3BX, UK*

²*Environment and Sustainability, College of Engineering, Mathematics and Physical Sciences, University of Exeter, Penryn, Cornwall, TR10 9EZ, UK*

³*School of Engineering and Physical Sciences, Heriot Watt University, Edinburgh, EH14 4AS, UK*

Abstract: Polytetrafluoroethylene (PTFE) microfiltration membranes are commonly used in Membrane Distillation (MD) systems, and parameters such as the pore size and porosity have significant influence on their performance. The operating temperature of a membrane distillation unit is typically 60-80°C, and while PTFE is considered to be thermally stable it does expand with increasing temperature. When dealing with a porous microstructure this expansion becomes significant. It was found that increasing the membrane temperature resulted in an expansion of the fibrous PTFE material and subsequently an increase in pore size. The membrane structure was observed over a period of 80 minutes, this time was deemed necessary given that PTFE has low thermal conductivity and therefore would heat up slowly. Pore size increased by 32% in the first 60 minutes, when the sample was heated to 80°C. A lumped system analysis of the heat transfer inside the SEM chamber was used to determine a heat transfer coefficient of 0.72 W/m²K. The temperature dependence of pore size will result in fluctuations in performance when the membrane is used intermittently and therefore heated and cooled periodically.

Keywords: PTFE Membranes, Membrane distillation, SEM, temperature, microstructure.

1. INTRODUCTION

Membrane distillation (MD) is an emerging thermally driven separation process, where vapor is transported across a hydrophobic microporous membrane. Compared with other separation processes, the MD process has advantageous characteristics such as 100% theoretical rejection of inorganic ions, macromolecules and other non-volatile compounds, insensitivity to feed concentration and low operating temperatures and pressures [1-3]. This process can be used for various applications such as seawater desalination, wastewater treatment and processing of food products [4]. The typical operating temperature range for MD is 60°C to 80°C [5]. Membrane distillation systems are increasingly being investigated for use with renewable energy sources, were intermittent use, and subsequent temperature changes are common. The effects of temperature on membrane structure is significant as it will influence its performance.

The most commonly used polymer in MD membranes is polytetrafluoroethylene (PTFE), these membranes were originally intended for microfiltration purposes [6]. Several groups have used image

analysis techniques to further understand the structure of microporous membrane material. Calvo *et al.* [7] used a Scanning Electron Microscopy (SEM) to image the surface of a polycarbonate membrane; this image was then analysed to determine the pore size distribution in the membrane. The method yielded values of mean pore size that were in agreement with the nominal data provided by the manufacturer. It also gave insight into the range of pore sizes in the membrane, resulting in a better understanding of the structure of the membrane which could in turn be used to more accurately predict performance characteristics such as flow rates and retention.

PTFE is generally considered to be thermally stable within the range of operating temperatures used in MD [8]. However, PTFE expands when heated [9]. In the context of microporous material such expansion could have a significant effect on the structure of the membrane. Changes in microstructure of the membrane as a result of temperature variations will affect the operating performance of the membrane. For example, the size and structure of the pores determine the mechanism of vapour diffusion across the membrane, and therefore the volume of distillate produced during operation. Li *et al.* [10] demonstrated that for membranes of the same thickness, the water vapor flux increased with increasing membrane pore size. The pore geometry also influences the Liquid

*Address correspondence to this author at the School of Engineering, University of Liverpool, Liverpool, L69 3BX, UK;
E-mail: amanda.hughes2@liverpool.ac.uk

Entry Pressure (*LEP*) of the membrane and therefore any changes would affect its hydrophobic properties. Xu *et al.* [11] examined the effect of membrane characteristics on air gap membrane distillation performance. They observed that larger pore size led to pore wetting due to lower *LEP*. Saffarini *et al.* [12] investigated the effects of temperature on the *LEP* of PTFE membranes under MD conditions. A decrease in *LEP* with temperature was observed, this was attributed to the decrease in both surface tension and contact angle as the temperature of the membrane increased. In addition, evidence of microstructure evolution as a function of temperature was observed and this was attributed to distortions in the fibril strands of PTFE.

Several studies have previously determined the heat transfer coefficients across the membrane and feed side membrane surface temperature, for varying operating conditions [13, 14]. However, the temperature of the membrane is difficult to measure, thermocouples placed on the membrane surface will also be in direct contact with the feed flow and therefore do not give an accurate measurement for the bulk membrane temperature. In this research, the microstructure of PTFE membrane samples was investigated at temperatures ranging from 17°C and 80°C. Image analysis was carried out to determine the effects of temperature on membrane pore size. The time taken for the sample to heat up and the pore size to become stable was investigated; the change temperature of the membrane over time and the heat transfer coefficient were calculated.

2. IMAGING PTFE MICROFILTRATION MEMBRANES

The membranes investigated in this study are GoreTM Microfiltration Media. The active side of the membrane is made of expanded PTFE and the support layer is woven polypropylene. The manufacturer states that the membranes have an average pore diameter of 0.2 µm, a porosity of 80% and a typical thickness of 0.24 mm.

The microstructure of PTFE membranes was investigated using a SEM. The SEM emits a focused beam of electrons which are directed at the sample; these electrons interact with the atoms in the sample causing it to emit a signal, and this signal can be measured to give information about the sample's topography. For the SEM process to work, the sample must be electrically conductive, therefore the PTFE membrane samples were coated with a layer of gold

5µm thick before they were imaged [15]. Images of the PTFE membrane at ambient temperature were taken at Heriot-Watt University's Centre for Microscopy. An FEI Quanta 3D SEM was used with a field emission source. In order to image the membrane samples at high temperature, an Environmental Scanning Electron Microscope (*E-SEM*) was used at the Laboratory for In-situ Microscopy and Analysis (*LIMA*) at the University of Oxford. A Carl Zeiss EVO LS15 E-SEM equipped with a LaB6 electron source was used, the set up at LIMA is shown in Figure 1.



Figure 1: E-SEM equipment set up at LIMA, University of Oxford.

The E-SEM is equipped with a Deben Coolstage inside of the SEM chamber, which consists of a Peltier stage with an operating temperature range of -25°C to +150°C. The temperature display has a resolution of 0.1°C and a maximum heating rate of 100°C/min. A layer of thermal paste was applied to a 10x10mm membrane sample to ensure good thermal contact with the stage, and the sample was placed on to the stage at room temperature. The SEM chamber was sealed, and an image was taken at room temperature. The stage was then set to a temperature within the operating range of MD process using external digital controls. Given its high heating rate, the stage reached the set temperature in under a minute. The temperature of the sample could not be directly measured inside of the chamber, however the temperature of the stage was measured and recorded throughout the experiment. The membrane structure was observed over a period of 80 minutes. This time was deemed necessary given that PTFE has low thermal conductivity and therefore would heat up slowly. Images from the SEM and E-SEM were analysed to determine pore size and porosity using ImageJ 1.48 software. The threshold function was used

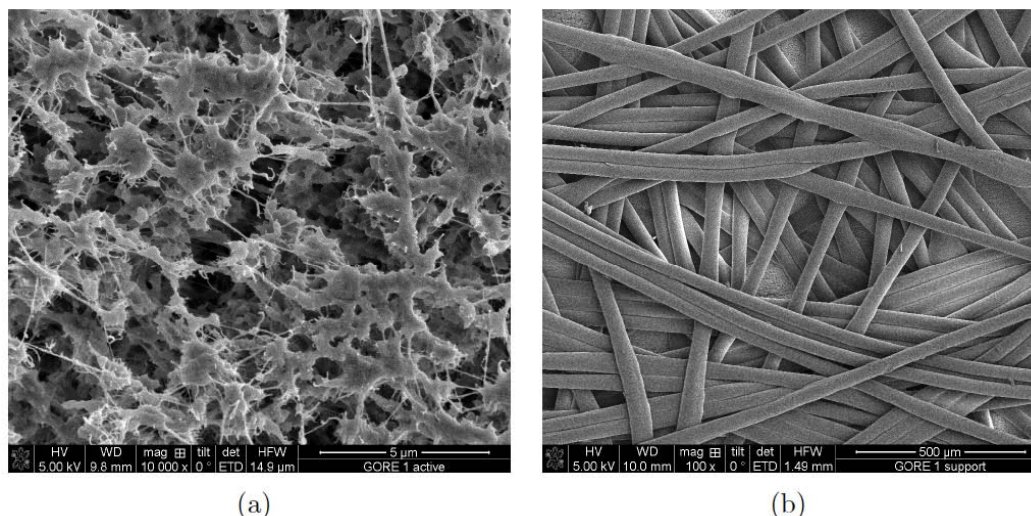


Figure 2: SEM image of **a)** active expanded PTFE membrane and **b)** woven polypropylene support layer.

to analyse porosity of the membrane. The Wand tracing function and Region Of Interest (*ROI*) manager tool were used to select and measure individual features on the images to determine pore size [16].

3. MEMBRANE MICROSTRUCTURE AT AN AMBIENT TEMPERATURE

The microstructure of GoreTM PTFE membranes was examined at a constant temperature of 17°C with the use of a SEM. The active layer of the membrane, made from expanded polytetrafluoroethylene (PTFE), can be seen in Figure 2a. The sample shows an uneven distribution of pore sizes across a non-uniform surface structure, where larger sections of material are connected to each other via thinner strands. Underneath the PTFE is a woven polypropylene support layer, shown in Figure 2b.

The porosity of the membrane, ϕ , is defined as [17]:

$$\phi = 1 - \frac{A_v}{A_m}, \quad (1)$$

where A_v is the total area of the pores and A_m is the total membrane surface area.

To determine the porosity of the membrane the image obtained from the SEM is digitised using ImageJ software and each pixel given a value on a greyscale between 0 - 255; the darkest pixels have a 0 value and the lightest have a value of 255. A threshold of 60 was set and every value above determined to be membrane material. This was done visually as this value which best selected all of the area that appeared to be

membrane material. The pixels identified as membrane material are counted to determine the porosity. Figure 3 shows the membrane material after the threshold was set, with the lighter pixels coloured red. Using this method, the porosity was found to be 84%±5. When considering the margin for error, the value of porosity determine via image analysis is similar to 80% stated in the manufacturer's specifications.

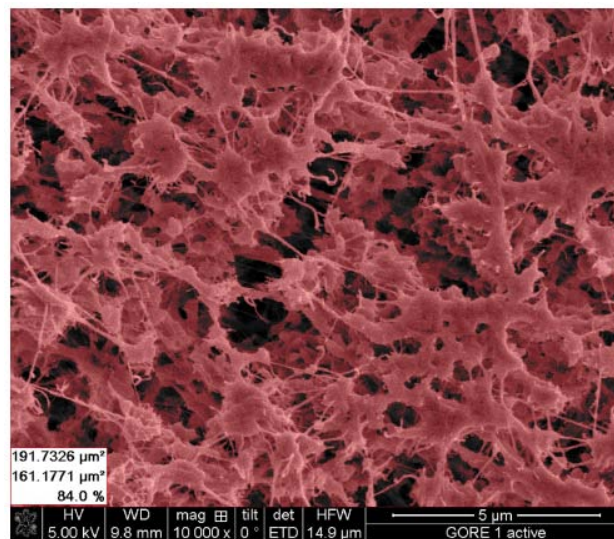


Figure 3: PTFE membrane with lighter pixels, considered to be membrane material, highlighted in red. Total surface area, total area of the membrane material and porosity are given in the bottom left, respectively.

The pore size was determined by the manufacturer through the use of capillary flow porometry, where a fully wetted sample of the membrane is put in a sealed chamber, compressed gas flows into the chamber and the pressure gradually increases until all of the liquid is forced out of the membrane pores. The pressure and

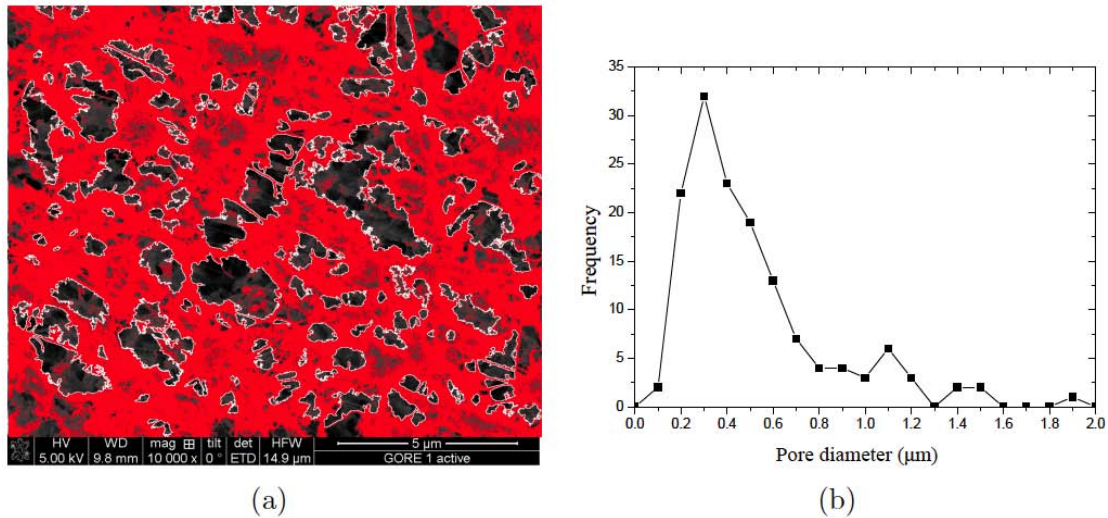


Figure 4: a) SEM image of PTFE membrane with selected pores perimeter highlighted in white and b) Equivalent pore diameter frequency distribution of the sample.

flow rates are recorded and used to calculate the pore size. These calculations assume that all pores are circular in cross section and uniform along their length. However, as Figure 2a shows, the membrane material is a complex web of interconnecting strands and fibres, that display little uniformity.

The SEM image was analysed and the perimeter and the area of each pore within the sample was measured. Although the pores are not circular, a representative value of pore diameter can be found using an equation for the equivalent pore diameter, d_p , which is defined as [18]:

$$d_p = 2\sqrt{\frac{A_p}{\pi}}, \quad (2)$$

where A_p is the area of the pore.

The software was used to select and measure 145 features in the image, identified as pores, these pores are highlighted in Figure 4a. There is a large variation in the area and equivalent diameters of the pores in the sample, ranging from 0.12–1.88 μm. The frequency distribution of pore diameters within the sample is shown in Figure 4b. The most frequently occurring pore diameter within the sample is 0.3 μm. This value is higher than the 0.2 μm average pore size stated by the manufacturer. The pores greater than 1 μm will have a much lower liquid entry pressure which may result in membrane wetting.

Both the values for porosity and pore diameter determined through image analysis are slightly larger than the manufacturer's specifications. This could be

due, in part, to the uneven distribution of pores across the surface of the membrane, highlighted in Figure 5 which shows the SEM image of the same membrane at a lower magnification. The image analysis presented was carried out on the bottom left region of the membrane highlighted as A; this region is particularly porous when compared to the region in the centre of the image. Another issue may be that the SEM image gives a 2-dimensional projection of the pores, the porosity is based on the top surface of the membrane which does not take account of the tortuosity of the pores and any structural changes that may exist through the cross section of the membrane.

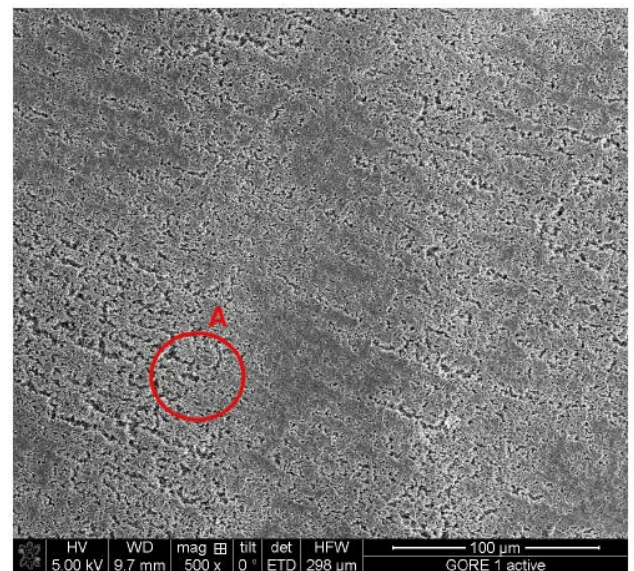


Figure 5: PTFE membrane surface at 500x magnification, highly porous region used in the analysis is circled and indicated as A.

4. MEMBRANE MICROSTRUCTURE AS A FUNCTION OF TEMPERATURE

The membranes used in these experiments have a complex structure; the pores are formed by interconnecting fibrous strands of PTFE material. The pore size distribution of PTFE membranes is usually assumed to be constant over the typical operating range of the MD process, from 60 - 80°C. However, PTFE is a thermoplastic, known to expand when heated. Therefore, as the membrane is heated, the fibrous strands will expand in all directions and the pore size will change. Pore size influences the performance of the membrane, as it effects factors such as LEP and the likelihood of membrane wetting. It also determines the mechanism of diffusion of vapour across the membrane and hence the volume of distillate produced.

PTFE is a synthetic semicrystalline fluoropolymer commonly known as Teflon. The PTFE molecule is highly stable, it has high heat resistance, chemical resistance and its crystalline melting point is 327°C [19]. It undergoes a crystal-crystal transition at 19.2°C and 34.5°C, when the average distance between molecules in its polymer chain increases [20]. This results in a rapid expansion of the material. Blumm *et al.* [9] measured the linear thermal expansion and expansivity of PTFE, shown in Figure 6. The linear thermal expansion coefficient, α , is defined by Kirby *et al.* [21] as:

$$\alpha = \frac{1}{L_0} \frac{\delta L}{\delta T}, \quad (3)$$

where L_0 is the original length of the sample, δL is the increase in length for an increase of δT in temperature.

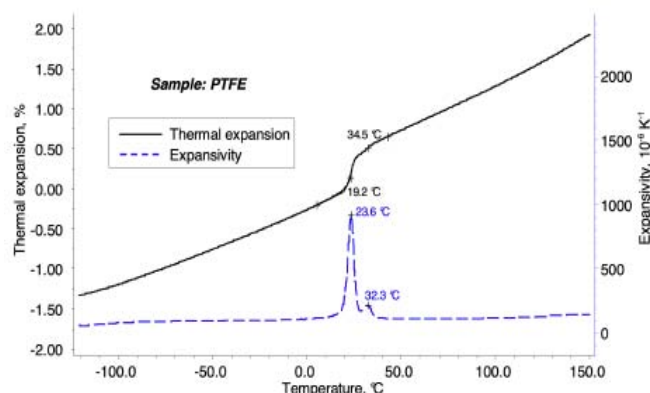


Figure 6: Thermal expansion and expansivity of PTFE material [9], (Reproduced with permission from the copyright holder).

The thermal expansion of PTFE within the operating range of MD is reversible when the material is cooled. The structural change in PTFE that occurs during the crystal-crystal transitions at 19.2°C and 34.5°C is also reversible [21]. As operation of the membrane module begins the material will expand, when the module cools, during an overnight shut down for example, the material will contract, and the process will repeat the next time the module is operated.

A series of experiments were carried out to understand the influence of temperature on the expansion of PTFE material and the size of the pores. A Deben Peltier heating stage was placed inside an SEM chamber and the sample was put directly on the stage. The chamber, Peltier stage and sample all had an initial temperature of 17°C. The temperature of the stage was then set using external controls, and the stage reached its set temperature in under 20 seconds. It is expected that the PTFE sample would take much longer to heat, as it has low thermal conductivity. The sample was therefore imaged every 10 minutes to determine the expansion of the material and the length of time for it to reach the temperature of the stage. It should be noted that these experiments were not repeated using the same membrane sample, this is due to the prohibitive length of time for the sample to cool inside of the SEM chamber and difficulty in location the same feature multiple times.

A fibrous strand of PTFE within the membrane sample was selected at random and imaged over time as the sample was heated to 70°C. Figure 7a shows the sample at its initial temperature of 17°C. An image was taken at 10 minute intervals after the stage temperature was set and these images illustrate an increase in the strand length from 3.864 μm to 4.007 μm over a 60 minute period. Figure 7c shows the length of the node measured on the image at 10 minute intervals as it was heated. The length of the strand increased over time. It is also important to note the presence of an initial rapid expansion in the strand's length within the first ten minutes, which corresponds to the solid-state transition that takes place at 19.2°C. The gradient of the trend decreases between 10 and 20 minutes. It then increases again after 20 minutes, indicating the event of the second solid state transition at 34.5°C. After this time the rate of increase in length is linear.

4.1. Temperature Effects on Pore Diameter

The effects of thermal expansion of the material on pore size was investigated for the same sample as it

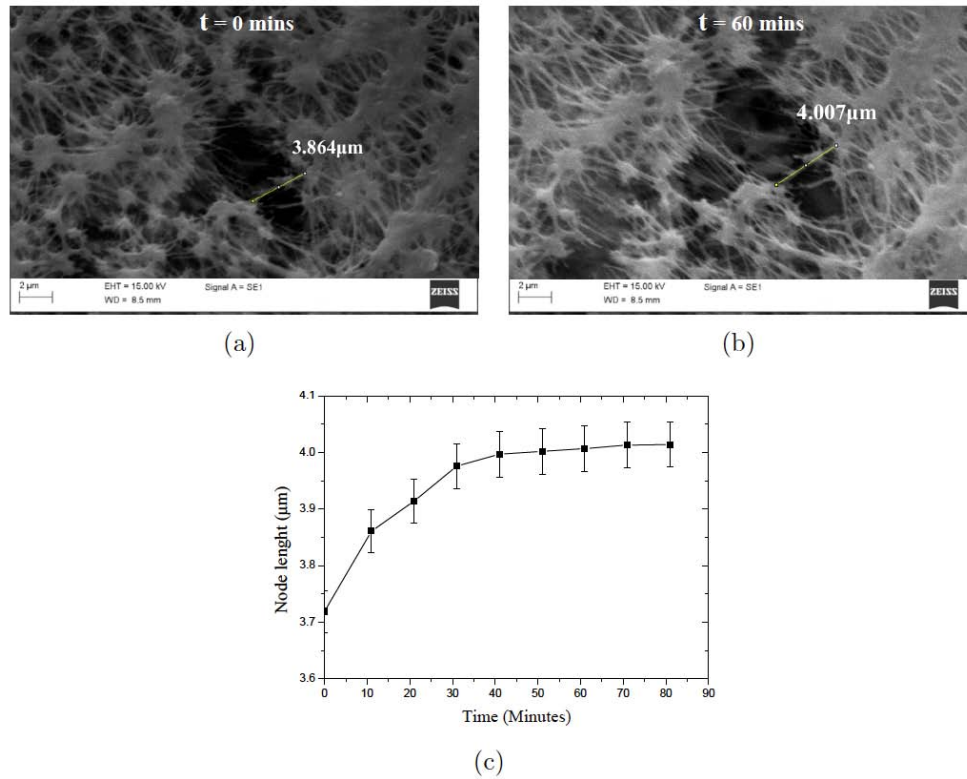


Figure 7: SEM images of a PTFE membrane when placed on a heating stages set at 70°C . The images show measurements of a strand at a) time 0 and b) 60 minutes, while c) shows the change in length of the strand when heated over an 80 minute period.

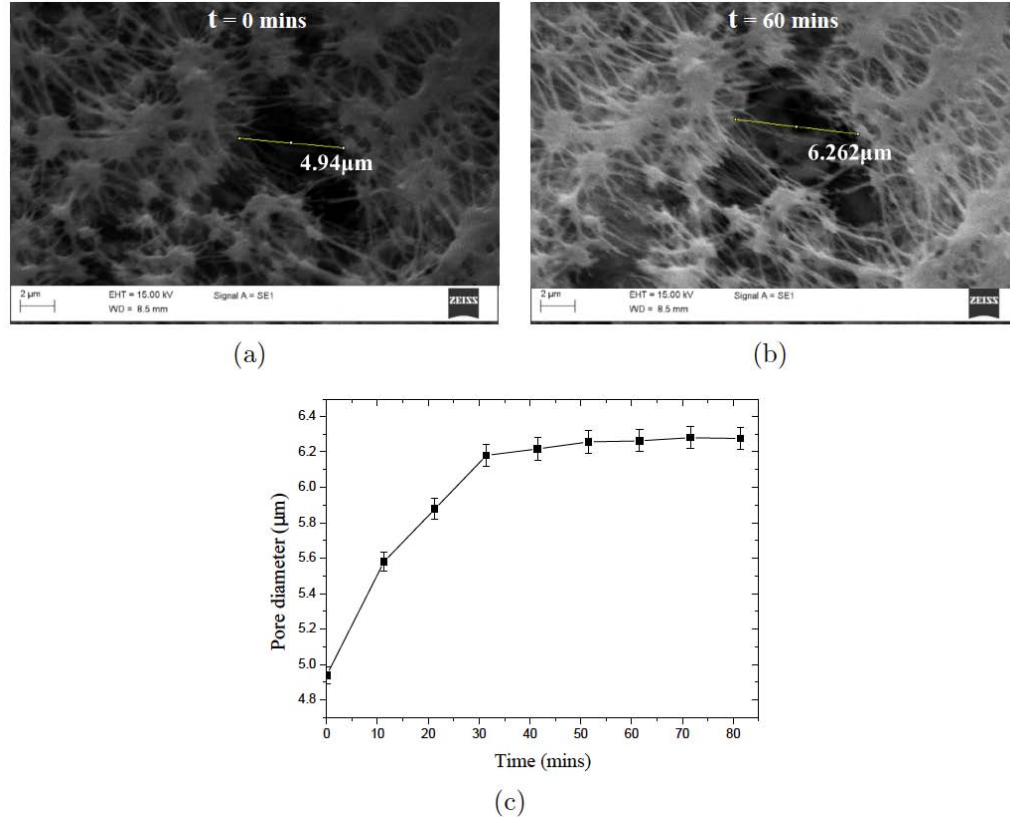


Figure 8: SEM images of a PTFE membrane when placed on a heating stages set at 70°C . The images show the pore diameter at time 0, then after 20, 40 and 60 minutes.

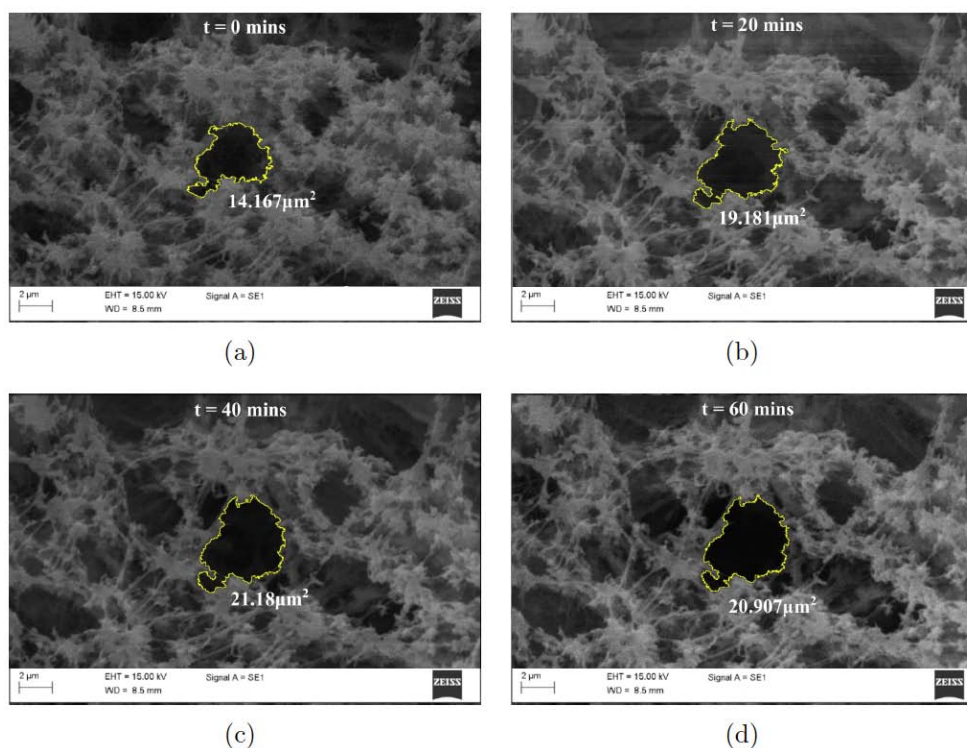


Figure 9: SEM images of a PTFE membrane when placed on a heating stages set at 80°C. The images show the pore at time 0, then after 20, 40 and 60 minutes. The pore perimeter is highlighted in each image.

was heated to 70°C. The membrane pores are not circular, therefore selecting the same diameter in each image is challenging. To overcome this, two distinct features on the perimeter of the pore are selected and a line segment drawn between them. The same features could then be easily identified and selected in the subsequent images, ensuring the same feature was measured throughout the analysis. Figure 8 shows pore length increase over time, at $t=0$ and 17°C the diameter of the pore was 4.94 μm, after 60 minutes the pore length had increased to 6.262 μm. This is due to thermal expansion of the strands of PTFE membrane material that make up the pore.

The pore expansion trend shown in the Figure 8c bears the same distinctive features as the trend for thermal expansion of PTFE, shown in Figure 6. There is an initial rapid expansion, corresponding to the transition phase at 19.2°C and a second rapid expansion corresponding to the second crystal-crystal transition at 34.5°C. After 40 minutes the diameter remained relatively constant, increasing by only 1%. From this we can assume that the sample reached a temperature approaching 70°C after 40 minutes.

To give an understanding of the pore's expansion in 2-dimensions, the area of the pore was measured when the sample was placed on the heating stage set

to 80°C and the wand tracing function in ImageJ software was used to select the perimeter of the pore. The SEM images are shown in Figure 9; the pore perimeter has been highlighted and a measurement for pore area is included on each image. Figure 9a shows that the area of the pore at room temperature was 14.167 μm². After 60 minutes, the area of the pore had increased to 20.907 μm², seen in Figure 9d; this is an increase of 32%. The area of the pore was measured at 10 minute intervals is shown in Figure 10. Figure 10 also shows the equivalent pore diameter, calculated using equation 2. There was an initial rapid increase in the area, followed by a period of linear expansion. The pore area becomes stable after 40 minutes, increasing by only 0.4% in the final 40 minutes of the experiment. Therefore, it is possible to infer that the pore's expansion is uniform in 2 dimensions.

A comparison of the rates of increase in equivalent pore diameter over time for samples heated to 60°C, 70°C and 80°C is shown in Figure 11. A different membrane sample was used each time, so in order to compare the material's rate of expansion for all three temperatures, the diameters measured for each sample were normalised and the dimensionless value of $\Delta \text{diameter}/\text{diameter}$ was compared. This figure shows that the rate of increase in the diameter of the pore is greatest when the Peltier stage was set to 80°C.

This is to be expected, as the temperature difference between the sample and the stage was greatest in this instance. The rate of increase was slowest when the stage was set to 60°C. In this case, the pore diameter had not stabilised after 80 minutes.

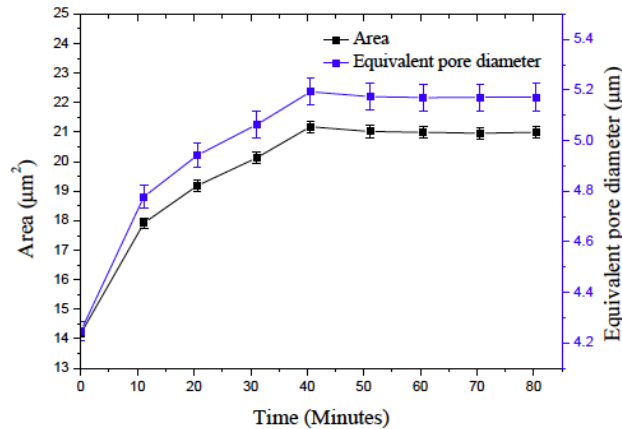


Figure 10: Increase in the area and equivalent diameter of the pore over time when heated to 80°C.

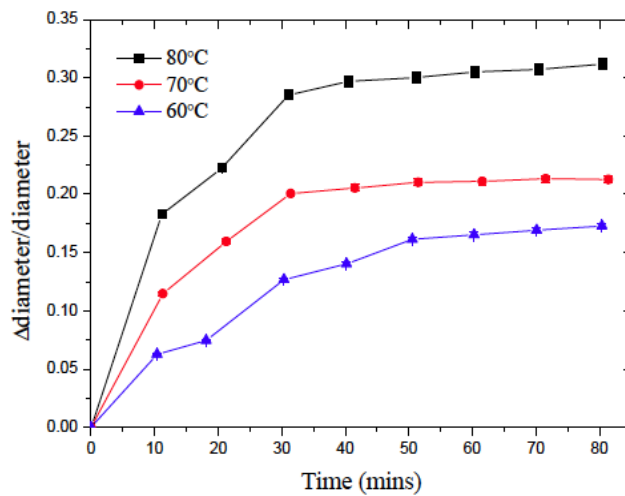


Figure 11: Normalised increase in equivalent pore diameter over time for samples heated to 60°C, 70°C and 80°C.

All the data presented here suggests that the membrane pores expand over time when heated, the higher the temperature the greater the overall increase in the size of the pores. Higher temperatures also give rise to a faster rate of expansion, due to a greater temperature gradient leading to a higher rate of heat transfer. Saffarini *et al.* [12] observed an increase in the average pore size of Gore PTFE membranes when annealed at higher temperatures. They also observed a decrease in the Liquid Entry Pressure (LEP) of the membrane at higher temperatures. LEP is defined as [5]:

$$LEP = \frac{-2B\gamma\cos(\theta)}{r_{max}}, \quad (4)$$

where B is a geometric factor that is determined by the pore's structure, γ is the surface tension of the liquid, θ is the contact angle between the liquid and the membrane surface and r_{max} is the maximum pore radius in the membrane; this is the pore most likely for liquid to enter. A decrease in LEP at higher temperatures is expected as surface tension and contact angle decrease with increasing temperature [22]. The LEP will also decrease as a result of thermal expansion of the pores. LEP should be greater than the trans-membrane pressure in the MD module to avoid membrane wetting. It was suggested by the Schneider *et al.* [23], that the pore diameter should not exceed 1 - 1.2 μm to avoid membrane wetting. However, Figure 4b shows that the membrane contains pore diameters greater than this value, 10% of the pores had diameter of 1 μm or above. This was prior to heating and thermal expansion, therefore, the increased pore diameter seen at higher temperatures will give greater risk of membrane wetting and hence increased conductivity of the distillate produced.

An increase in the average pore size of the membrane will also result in increased vapour diffusion across the membrane, and therefore greater distillate flux. The rate of expansion of membrane pores during operation within an MD module is expected to be larger than shown in this analysis, as the flux of vapour through the membrane pores will increase the rate of heat transfer to membrane material. Membrane wetting and water intrusion into the pores would also have a significant influence on pore dilation [12].

4.2. Theoretical Modelling of Heat Transfer Coefficients and Temperature of the PTFE Samples

A lumped system analysis of the heat transfer coefficients for the PTFE samples was carried out. A lumped system analysis can be undertaken on an object if the temperature throughout the object can be assumed to uniform [24]. Given that the membrane samples tested are relatively thin, approximately 0.24 mm, this assumption can be made without loss of accuracy. To determine the rate at which the temperature of the sample increased and to calculate the heat transfer coefficient for the PTFE membrane inside the SEM, a temperature curve was fitted to data for expansion of the pore shown in the previous section. The initial temperature inside of the SEM chamber was known to be 17°C, the final temperature

of the sample was assumed to be equal to the set temperature of the Peltier stage when the size of the pores in the sample had reached steady state.

An energy balance between the heat transferred to the sample during time interval dt and the increase in the energy of the sample during the same time interval can be expressed in the following equation [24];

$$hA_s(T_\infty - T)dt = mC_p dT. \quad (5)$$

Where m (kg) is the mass of the sample, A_s (m) is the area of the sample, C_p (J/kgK) is the specific heat capacity of the material and h (W/m²K) is the heat transfer coefficient. In this analysis T_∞ is the temperature of the Peltier stage on which the sample rests. The value for the mass of the sample is equal to;

$$m = \rho V \quad (6)$$

where ρ (kg/m³) is the density of the material and V is the volume of the sample. Noting that $dT = d(T - T_\infty)$ since T_∞ is always constant, equation 6 can be written as:

$$\frac{d(T - T_\infty)}{(T - T_\infty)} = -\frac{hA_s}{\rho VC_p} dt \quad (7)$$

Integrating between $t=0$ when $T = T_i$ to time $t=t$ when $T = T(t)$, gives the following equation:

$$\ln \frac{T(t) - T_\infty}{T_i - T_\infty} = -\frac{hA_s}{\rho VC_p} t \quad (8)$$

Taking the exponential of both sides gives;

$$\frac{T(t) - T_\infty}{T_i - T_\infty} = e^{-bt} \quad (9)$$

where:

$$b = -\frac{hA_s}{\rho VC_p} \quad (10)$$

b is the reciprocal of the time constant and has the units s^{-1} .

By using equation 9, the temperature of a sample after time, t , can be determined. As this is an exponential function, the temperature of the sample will increase rapidly at first, and later slow down. This equation can be used to calculate the amount of time taken for the sample to reach T_∞ . Altering the value of

b changes the curvature of the trend, the larger the value b , the greater the rate of heat transfer, therefore the sample reaches T_∞ in a shorter time.

Values of b were selected to fit the curve of $T(t)$ against time, t , to the trends of pore expansion shown in the previous section. T_i is 17°C in all cases, as this is the initial temperature inside the SEM chamber after the vacuum is applied. To investigate the increase in temperature when the Peltier stage was set to 80°C, the trend shown in Figure 11 was used and 80°C was used as the value for T_∞ . The value of b varied, for each 10 minute interval in order to fit exactly to the trend for increase in the pore diameter. Figure 12 shows how the value of b obtained from this method varied over the course of the 80 minute experiment.

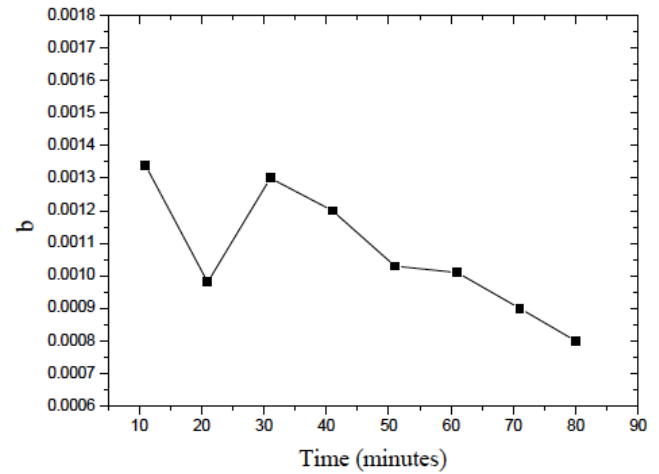


Figure 12: Values for b over time, when $T_\infty = 80^\circ\text{C}$.

A single value of b was obtained by taking the average of the first four points on the graph. This method was preferred as the uncertainty in b increases greatly as the $T(t)$ approaches T_∞ , as the ΔT between time intervals decreases. For this analysis the average value of b was found to be 1.21×10^{-3} . It is important to note that the peaks seen at 10 minutes and 30 minutes correspond to the periods of rapid expansion in the PTFE material believed to be the result of the phase transitions that occur at 19.2°C and 34.5°C. This accelerated period of expansion therefore does not correspond to a similarly rapid increase in the temperature of the sample. This effect was lessened by taking an average value of b .

By substituting values for the specific heat capacity and density of PTFE, along with the area and volume of the sample into equation 12 and rearranging, the heat transfer coefficient, h , was obtained. When calculating the volume of material, the percentage

porosity was also taken into account. The following equation was used;

$$V_{\text{sample}} = A_m * \delta_{\text{membrane}} * \phi, \quad (11)$$

Table 1: Properties of the Gore™ PTFE Samples

property	value	units
Specific heat capacity, C_p	1090	J/kg K [25]
Density, ρ	2200	kg/ m^3 [3]
Area, A	2.5×10^{-5}	m^2
Volume, V	5.04×10^{-9}	m^3

where δ_{membrane} (mm) is the thickness, A_m is the area and ϕ is the porosity of the membrane, as defined in equation 1. The relevant PTFE material properties are shown in Table 1. Using these values and the average value of b , the heat transfer coefficient, h , was found to be $0.72 \text{ W/m}^2\text{K}$. This value for heat transfer coefficient is low, as expected, considering the relatively high heat capacity of a thermoplastic such as PTFE and given that it took 80 minutes for $T(t)$ to increase to a value near to T_∞ . Also, poor contact between the membrane and the stage could be a factor.

Figure 13 shows a plot of $T(t)$ against time for T_∞ equal to 80°C , calculated using the average value of b for the first 40 minutes, 1.21×10^{-3} . The figure also shows the expansion of the pore diameter divided by the original pore length over time. The curve produced when using the average value of b gives a lower value of $T(t)$ at 10 and 30 minutes, than the corresponding point on the $\Delta \text{Diameter}/\text{diameter}$ curve.

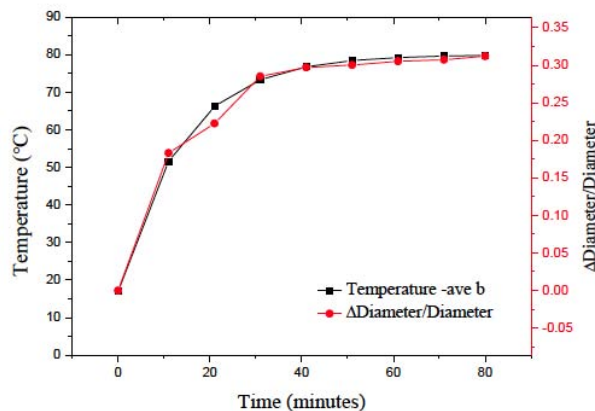


Figure 13: Temperature of the membrane sample over time when $T_\infty = 80^\circ\text{C}$, based on average value of b and a heat transfer coefficient of $0.72 \text{ W/m}^2\text{K}$.

5. CONCLUSIONS

This research investigates membrane microstructure at temperatures up to 80°C , the maximum operating temperature of MD process. To establish a baseline, the structure of the membrane was examined at an ambient temperature of 17°C . SEM image analysis was used to measure the porosity of the sample, which was found to be $84 \pm 4\%$. This value was comparable to the porosity value of 80% stated by the manufacturer, which was determined by capillary flow porometry. Analysis of the membrane under magnification showed that the pores are not regular in shape and are also not evenly distributed across the surface of the membrane. The sample shows an uneven distribution of pore sizes across the surface, with larger sections of material connected to each other via thinner strands. A large variation in the size of the pores within the sample was observed. Pore sizes ranged from $0.12 - 1.88 \mu\text{m}$, and the average value was $0.51 \pm 0.32 \mu\text{m}$. However, a frequency distribution analysis gave a modal value of $0.3 \mu\text{m}$, closer to the $0.2 \mu\text{m}$ quoted by the manufacturer.

An E-SEM fitted with a Peltier stage and temperature controls was used image the membrane at a range of temperatures from $17^\circ\text{C} - 80^\circ\text{C}$. It was found that the pores expanded over time when heated, this is thought to be a result of the thermal expansion of PTFE material. Logically one may assume that an expansion in the PTFE material would result in smaller pores, however, the membrane was found to have a fibrous microstructure, therefore as the material heated the strands of PTFE expanded resulting in larger pore sizes. The largest increase in pore diameter was seen when the sample was heated to 80°C , the equivalent pore diameter increased by 32% over a 60 minute period. This change in pore size as a result of temperature will influence membrane performance. When used in the MD process larger pores would result in an increased diffusion of vapour across the membrane resulting in larger distillate flux. However, an increase in pore size will also reduce the liquid entry pressure of the pores and could result in membrane wetting, resulting in feed solution leaking into the distillate.

A lumped system analysis of the heat transfer inside the SEM chamber was used to determine a heat transfer coefficient of $0.72 \text{ W/m}^2\text{K}$, when a membrane sample was heated to 80°C . From this analysis the relationship between increase in temperature and increase in pore length was

established. Therefore, we can conclude that the change in membrane temperature during intermittent use and subsequent change in the pore size will influence the performance of an MD module. When a membrane module is shut down for an overnight period, as is the case with solar powered MD systems for example, the temperature of the membrane will decrease to ambient. When operation begins the next day, the membrane will be heated to the temperature of the feed causing the pores to expand. This change in pore size will influence the quantity and the quality of the distillate yield and should be investigated further.

REFERENCES

- [1] El-Bourawi MS, Ding Z, Ma R, Khayet M. A framework for better understanding membrane distillation separation process. *Journal of Membrane Science* 2006; 285(1–2): 4-29. <https://doi.org/10.1016/j.memsci.2006.08.002>
- [2] Khayet M, Matsuura T. *Membrane distillation: Principles and applications*. Elsevier, 2011; chapter 15: 437. <https://doi.org/10.1016/B978-0-444-53126-1.10011-9>
- [3] Wang P, Chung T-S. Recent advances in membrane distillation processes: Membrane development, configuration design and application exploring. *Journal of Membrane Science* 2015; 474: 39-56. <https://doi.org/10.1016/j.memsci.2014.09.016>
- [4] Alkhdhiri A, Darwish N, Hilal N. Membrane distillation: A comprehensive review. *Desalination* 2012; 287: 2-18. Special Issue in honour of Professor Takeshi Matsuura on his 75th Birthday. <https://doi.org/10.1016/j.desal.2011.08.027>
- [5] Lawson KW, Lloyd DR. Membrane distillation. *Journal of Membrane Science* 1997; 124(1): 1-25. [https://doi.org/10.1016/S0376-7388\(96\)00236-0](https://doi.org/10.1016/S0376-7388(96)00236-0)
- [6] Qtaishat MR, Banat F. Desalination by solar powered membrane distillation systems. *Desalination* 2013; 308: 186-197. *New Directions in Desalination*. <https://doi.org/10.1016/j.desal.2012.01.021>
- [7] Calvo JI, Hernandez A, Caruana G, Martinez L. Pore size distributions in microporous membranes: I. surface study of track-etched filters by image analysis. *Journal of Colloid and Interface Science* 1995; 175(1): 138-150. <https://doi.org/10.1006/jcis.1995.1439>
- [8] Feng S, Zhong Z, Wang Y, Xing W, Drioli E. Progress and perspectives in ptfе membrane: Preparation, modification, and applications. *Journal of Membrane Science* 2018; 549: 332-349. <https://doi.org/10.1016/j.memsci.2017.12.032>
- [9] Blumm J, Lindemann A, Meyer M, Strasser C. Characterization of ptfе using advance thermal analysis techniques. *International Journal of thermophysics* 2008; 31: 1919-1927. <https://doi.org/10.1007/s10765-008-0512-z>
- [10] Li L, Sirkar KK. Influence of microporous membrane properties on the desalination performance in direct contact membrane distillation. *Journal of Membrane Science* 2016; 513: 280-293. <https://doi.org/10.1016/j.memsci.2016.04.015>
- [11] Xu J, Singh YB, Amy GL, Ghaffour N. Effect of operating parameters and membrane characteristics on air gap membrane distillation performance for the treatment of highly saline water. *Journal of Membrane Science* 2016; 512: 73-82. <https://doi.org/10.1016/j.memsci.2016.04.010>
- [12] Saffarini RB, Mansoor B, Thomas R, Ararat HA. Effect of temperature-dependent microstructure evolution on pore wetting in {PTFE} membranes under membrane distillation conditions. *Journal of Membrane Science* 2013; 429(0): 282-294. <https://doi.org/10.1016/j.memsci.2012.11.049>
- [13] Gryta M, Tomaszewska M, Morawski AW. Membrane distillation with laminar flow. *Separation and Purification Technology* 1997; 11(2): 93-101. [https://doi.org/10.1016/S1383-5866\(97\)00002-6](https://doi.org/10.1016/S1383-5866(97)00002-6)
- [14] Ali A, Macedonio F, Drioli E, Aljil S, Alharbi OA. Experimental and theoretical evaluation of temperature polarization phenomenon in direct contact membrane distillation. *Chemical Engineering Research and Design* 2013; 91(10): 1966-1977. The 60th Anniversary of the European Federation of Chemical Engineering (EFCE). <https://doi.org/10.1016/j.cherd.2013.06.030>
- [15] Goldstein JI, Newbury DE, Echlin P, Joy DC, Fiori C, Lifshin E. *Scanning electron microscopy and x-ray microanalysis. a text for biologists, material scientists and geologists*. kluwer academic 1981. <https://doi.org/10.1007/978-1-4613-3273-2>
- [16] Schneider CA, Rasband WS, Eliceiri KW. Nih image to imagej: 25 years of image analysis. *Nature Methods* 2012; 9(7): 671-675. <https://doi.org/10.1038/nmeth.2089>
- [17] Schock G, Miguel A. Mass transfer and pressure loss in spiral wound modules. *Desalination* 1987; 64: 339-352. [https://doi.org/10.1016/0011-9164\(87\)90107-X](https://doi.org/10.1016/0011-9164(87)90107-X)
- [18] Hernández A, Calvo JI, Prádanos P, Palacio L, Rodríguez ML, de Saja JA. Surface structure of microporous membranes by computerized sem image analysis applied to anopore filters. *Journal of Membrane Science* 1997; 137(1-2): 89-97. [https://doi.org/10.1016/S0376-7388\(97\)00184-1](https://doi.org/10.1016/S0376-7388(97)00184-1)
- [19] Brydson JA. *Plastics materials*. Butterworth-Heinemann Ltd, Fifth edition 1989; 344.
- [20] Engeln I, Hengl R, Hinrichsen G. Thermal expansion and youngs modulus of uniaxially drawn ptfе in the temperature range 100 to 400 k. *Colloid and polymer science* 1984; 262: 780-787. <https://doi.org/10.1007/BF01451707>
- [21] Kirby R. Thermal expansion of polytetrafluoroethylene (teflon) from -190 to 300 celsius. *Journal of research of the national bureau of standards* 1956; 57(91). <https://doi.org/10.6028/jres.057.010>
- [22] Garca-Payo MC, Izquierdo-Gil MA, Fernández-Pineda C. Wetting study of hydrophobic membranes via liquid entry pressure measurements with aqueous alcohol solutions. *Journal of Colloid and Interface Science* 2000; 230(2): 420-431. <https://doi.org/10.1006/jcis.2000.7106>
- [23] Schneider K, Hölz W, Wollbeck R, Ripperger S. Membranes and modules for transmembrane distillation. *Journal of Membrane Science* 1988; 39(1): 25-42. [https://doi.org/10.1016/S0376-7388\(00\)80992-8](https://doi.org/10.1016/S0376-7388(00)80992-8)
- [24] Cengel Y. *Heat transfer: A practical approach*. McGraw-Hill, 2003; Chapter 4: 218-220.
- [25] Subodh G, Manjusha MV, Philip J, Sebastian MT. Thermal properties of polytetrafluoroethylene/sr2ce2ti5o16 polymer/ceramic composites. *Journal of Applied Polymer Science* 2008; 108(3): 1716-1721. <https://doi.org/10.1002/app.27606>